ATM and MET kinases are synthetic lethal with non-genotoxic activation of p53

Kelly D. Sullivan[1], **Nuria Padilla-Just**[1], **Ryan E. Henry**[1], **Christopher C. Porter**[2], **Jihye Kim**[3], **John J. Tentler**[3], **S. Gail Eckhardt**[3], **Aik Choon Tan**[3], **James DeGregori**[2,4], and **Joaquín M. Espinosa**[1,*]

[1]Howard Hughes Medical Institute & Department of Molecular, Cellular and Developmental Biology, University of Colorado at Boulder

[2]Department of Pediatrics, University of Colorado at Denver Anschutz Medical Campus

[3]Department of Medicine/Medical Oncology, University of Colorado at Denver Anschutz Medical Campus

[4]Department of Biochemistry and Molecular Genetics, University of Colorado at Denver Anschutz Medical Campus

Abstract

The p53 tumor suppressor orchestrates alternative stress responses including cell cycle arrest and apoptosis, but the mechanisms defining cell fate upon p53 activation are poorly understood. Several small molecule activators of p53 have been developed, including Nutlin-3, but their therapeutic potential is limited by the fact that they induce reversible cell cycle arrest in most cancer cell types. We report here the results of a 'Synthetic Lethal with Nutlin-3' genome-wide shRNA screen, which revealed that the ATM and MET kinases govern cell fate choice upon p53 activation. Genetic or pharmacological interference with ATM or MET activity converts the cellular response from cell cycle arrest into apoptosis in diverse cancer cell types without affecting expression of key p53 target genes. ATM and MET inhibitors enable Nutlin-3 to kill tumor spheroids. These results identify novel pathways controlling the cellular response to p53 activation and aid in the design of p53-based therapies.

The p53 tumor suppressor is a master regulator of the cellular response to various stresses including oncogene hyperactivation, DNA damage and nutrient deprivation. Upon activation, p53 participates in diverse cellular responses such as cell cycle arrest,

*To whom correspondence should be addressed: joaquin.espinosa@colorado.edu; FAX: (303) 492-7744.

Author Contributions

Competing Financial Interest.

senescence, autophagy and apoptosis[1]. Consequently, *TP53* is the most frequently mutated tumor suppressor gene in human cancer, with inactivating mutations occurring in ~50% of tumors. In the remaining cases, p53 function is abrogated by alternative oncogenic events such as hyperactivation of MDM2, the main repressor of p53. It is estimated that 11 million cancer patients worldwide carry tumors expressing wild type p53, creating a unique therapeutic opportunity to harness its tumor suppressive function for selective elimination of cancer cells[2].

Historically, the anti-tumoral effects of p53 have been exploited by therapeutic strategies using genotoxic drugs or ionizing radiation, and p53 mutation status often determines the efficacy of these strategies[3]. However, systemic administration of DNA damaging agents leads to cell death in many healthy tissues, as well as accumulation of DNA mutations that lead to secondary cancers later in life, which clearly limits their therapeutic benefits. As the paradigm of cancer treatment shifts from genotoxic agents to biologically targeted therapies and personalized medicine, p53 has become a prime target for novel drugs. Several non-genotoxic small molecule activators of p53 are now available, which act by binding p53, MDM2 or other p53 repressors[4]. A pioneering molecule in the field is Nutlin-3, which mimics three hydrophobic amino acids of p53 required for MDM2 binding, thus acting as a competitive inhibitor of the p53-MDM2 interaction[5]. Nutlin-3 treatment induces strong p53 stabilization and effective induction of p53 target genes. Unfortunately, Nutlin-3 treatment of most cell lines expressing wild type p53 results in reversible cell cycle arrest rather than apoptosis or senescence[6–8]. From a therapeutic perspective, transient cell cycle arrest is the least preferred outcome, as it would merely produce a temporary stalling of tumor growth *in vivo*. In several animal models mimicking therapeutic p53 activation within tumors, cancer cells were effectively cleared via induction of p53-dependent apoptosis and/or senescence[9,10]. Thus, as several small molecule activators of p53 enter clinical trials, their efficacy will remain tied to a basic scientific question: what determines the cellular response to p53 activation?

Cell fate choice upon p53 activation is both stimulus- and cell type-specific. In the absence of activating stimuli, p53 is constitutively transcribed and translated but rapidly targeted for degradation by the E3 ubiquitin ligase activity of MDM2. Additionally, MDM2 blocks the N-terminal transactivation domain of p53. Cellular stress leads to posttranslational modifications in both p53 and MDM2 that disrupt their interaction, thus stabilizing and activating p53[1]. Activated p53 acts in the nucleus as a potent transcriptional regulator of genes in diverse functional pathways. p53-dependent cell cycle arrest is mostly mediated by transactivation of CDK inhibitors including *CDKN1A* (p21)[11] and *SFN* (14-3-3σ) [12]. In contrast, p53-dependent apoptosis is mediated largely by transactivation of genes such as *BBC3*, which encodes the BH3-only protein PUMA[13,14], as well as induction of various genes in the death receptor pathway[15,16]. Despite many research efforts in this area, it remains unclear how exactly the p53 network determines cell fate choice in a context-dependent manner. The prevailing view is that differential regulation of CDK-inhibitors versus BH3-only proteins tips the balance toward cell cycle arrest or apoptosis, but many other mechanisms are also possible[17,18].

In order to gain new insights into the molecular mechanisms of cell fate choice upon p53 activation, we performed a genome-wide shRNA screen to identify modifiers of the cellular response to Nutlin-3 treatment. Specifically, we sought to identify gene modules that promote survival upon non-genotoxic activation of p53. In theory, such gene products could be targeted in a combinatorial fashion with Nutlin-3 to promote cell death. Importantly, our screen identified numerous pathways not previously known to affect the cellular response to p53 activation in this fashion. We focused on the signaling pathways governed by the protein kinases ATM and MET, which arose from our screen as strongly synthetically lethal with Nutlin-3-activated p53. In fact, we demonstrate that specific shRNAs and small molecules targeting ATM and MET can be combined with Nutlin-3 to convert cell fate choice upon p53 activation from cell cycle arrest to apoptosis. The *in vitro* efficacy of the combinatorial strategies is far superior to any of the agents in isolation. Mechanistic studies reveal that inhibition of ATM and MET does not affect p53-dependent activation of p21, 14-3-3σ, PUMA or BAX. However, inhibition of these kinases does enable activation of the extrinsic apoptotic pathway upon Nutlin-3 treatment. These results lead to a revision of the role of ATM in the p53 network, as this kinase is usually depicted as a p53 agonist in the context of a DNA damage response, and demonstrate the importance of the interaction between the MET and p53 pathways. This report also illustrates the power of functional genomics approaches to accelerate both our understanding of gene networks and the design of effective combinatorial strategies for cancer therapy.

RESULTS

A screen for 'Synthetic Lethal with Nutlin-3' genes

Previous work from our lab and others has established *in vitro* assays to study cell type- and stimulus-specific responses to p53 activation (Fig. 1a–e). Whereas treatment with Nutlin-3 triggers p53-dependent cell cycle arrest in HCT116 colorectal cancer cells and A549 lung cancer cells, identical treatment leads to apoptosis in BV173 chronic myelogenous leukemia cells[6,8]. However, p53-dependent apoptosis can be rapidly elicited in HCT116 cells by treatment with 5-fluorouracil (5FU)[19]. Intriguingly, p53 activation by Nutlin-3 leads to equivalent induction of the key apoptotic p53 target gene PUMA in all three cell lines, yet only BV173 cells display activation of executioner caspase 3 (Fig. 1c). These observations led us to hypothesize that pro-survival pathways protect HCT116 and A549 cells from the apoptotic effects of the p53-PUMA axis under conditions of non-genotoxic p53 activation. To identify these pathways in an unbiased fashion, we performed a genome-wide shRNA screen for genes that are Synthetic Lethal with Nutlin-3 (SLNs) (Fig. 1f). HCT116 and A549 cells were transduced with the SBI 200K shRNA lentiviral library and selected with puromycin. Cell cultures were propagated for seven days for clearance of those cells expressing shRNAs targeting essential genes from the population. Cells carrying the cleared library were then treated with Nutlin-3 or vehicle (DMSO) for seven days. During this time, we expected cells carrying shRNAs against SLNs to disappear from the Nutlin-3-treated population. In order to identify these shRNAs, we allowed cells to recover for one week after Nutlin-3 treatment, extracted total RNA, amplified shRNAs via RT-PCR with primers against vector sequences, and subjected the PCR products to Illumina DNA deep-sequencing (see Methods for details). In order to identify shRNAs differentially expressed in

the DMSO- versus Nutlin-3-treated cell populations, we developed a novel bioinformatics pipeline dubbed BiNGS (Bioinformatics for Next Generation Sequencing). Briefly, BiNGS takes into account: i) the fold change in shRNA expression between treatment groups, ii) the variability in shRNA read counts across biological replicates, and iii) the number of shRNAs targeting a given gene that display the same behavior (Supplementary Results, Supplementary Fig. 1a, see Methods for detailed description)[20,21].

BiNGS identified hundreds of shRNAs that were differentially expressed between DMSO- and Nutlin-3-treated HCT116 and A549 cells (Fig. 2a,b, Supplementary Figure 1b,c and Supplementary Datasets 1–4). Hierarchical analysis demonstrated efficient clustering of the DMSO and Nutlin-3 biological replicates for both cell types and predicted two groups of genes: SLNs (read counts in DMSO > Nutlin-3) and *'Nutlin-3-resistance'* genes (read counts in DMSO < Nutlin-3). From this point forward, we focused our efforts only on the SLN group. For validation purposes, we selected 30 SLN candidates that scored in both cell lines along a wide range of fold change values for individual shRNAs (Fig. 2c) as well as p(wZ) values (Fig. 2d). p(wZ) values integrate the information from multiple shRNAs targeting a single gene, thus minimizing the impact of possible 'off-target' effects (see Methods for p(wZ) calculation and selection criteria for the 30 validated genes). To further increase the stringency of our validation efforts, we employed shRNAs from a different library (TRC, The RNAi Consortium) than that employed in the screen (SBI library). Since the targeting sequences in the shRNAs from the TRC library are different than those in the SBI library, switching shRNA collections significantly increased our confidence in positively validated genes. We created cell lines stably expressing individual shRNAs against candidate SLNs and determined their viability after Nutlin-3 treatment relative to: a) the respective DMSO control, and b) a control cell line expressing a non-targeting shRNA (Fig. 2e). We found that 18/30 candidate SLNs displayed <50% relative viability and 24/30 showed <75% relative viability.

Taken together, these observations indicate that our screening approach successfully identified many novel genes that promote survival upon p53 activation by Nutlin-3.

Pathway analysis highlights key synthetic lethal nodes

To select specific SLNs for further investigation, we sought out the signaling pathways most significantly represented among our top ranked screen hits. We reasoned that the biological relevance of individual SLNs should be stronger if several other components of the same pathway also display synthetic lethality. To identify these master SLN pathways, we subjected the top ~500 SLNs (p(wZ) <0.005) from HCT116 cells to IPA analysis (Ingenuity Systems, www.ingenuity.com) (Fig. 3). Interestingly, subsequent to the generic *'Molecular Mechanism of Cancer'* pathway, the top four pathways have been clearly implicated in the progression of colorectal carcinomas: Hepatic Growth Factor (HGF)/MET pathway[22], Cholecystokinin/Gastrin-mediated signaling[23], Interleukin 8 (IL8) pathway[24] and ATM signaling pathway[25]. Comparison of the components of these top five pathways revealed significant crosstalk among them with numerous genes being associated with multiple pathways, such as the multifunctional stress associated protein kinase (SAPKs) MAPK9, MAPK12, and MAP2K4 (Fig. 3a). Based on four criteria, we chose to focus on the ATM

and HGF/MET signaling modules, which contain at least eight close interactors displaying strong synthetic lethality (Fig. 3b,c). First, shRNAs against both kinases and at least one other member within the same pathway produced strong synthetic lethality during validation efforts (Fig. 2e). Second, small molecule inhibitors are available for both kinases, which could lead us to chemical strategies to modulate the cellular response to p53 activation. Third, ATM is often depicted as an agonist of p53 activity during the DNA damage response, yet our screen indicates that it functions as an antagonist of p53-dependent cell death in Nutlin-3-treated cells. Fourth, MET is a potent oncogene in colorectal cancer and other malignancies, and a role in suppression of p53-dependent cell death could provide a mechanistic basis for its oncogenicity.

ATM inhibition promotes p53-dependent apoptosis

The synthetic lethality of ATM with Nutlin-3 was confirmed by testing the impact of 15 different ATM shRNAs on HCT116 cells (Supplementary Fig. 2a). In fact, all of these shRNAs lead to decreased cell viability upon Nutlin-3 treatment relative to a non-targeting shRNA, with a clear correlation between the degree of knockdown and the impact on cell viability. We selected shRNAs #6 and #12, which show the strongest knockdown and the greatest effect on viability for further studies. Of note, these shRNAs reduce viability upon p53 activation to an extent comparable to an shRNA targeting the pro-survival factor BCL2, a potent antagonist of PUMA and other BH3-only proteins (Fig. 4a). In fact, ATM knockdown leads to an increase in apoptosis upon Nutlin-3 treatment that is comparable to that observed upon BCL2 knockdown (Fig. 4b). ATM knockdown also leads to increased apoptosis in Nutlin-3-treated A549 cells (Supplementary Fig. 3). Next, we tested whether pharmacological inhibition of ATM could recapitulate the synthetic lethal phenotype. Strikingly, combined treatment of HCT116 cells with Nutlin-3 and the ATM-specific inhibitor KU-55933[26] (hereafter referred to as ATMi) results in activation of executioner caspase 3 and apoptotic cell death comparable to that seen with the chemotherapeutic agent 5FU, a strong elicitor of p53-dependent cell death[19] (Fig. 4c,d). Importantly, neither Nutlin-3 nor ATMi in isolation activate caspase 3 or trigger substantial cell death. The efficacy of the combination treatment is also obvious in clonogenic survival assays (Supplementary Fig. 2b). Apoptosis caused by the combination treatment is both caspase- and p53-dependent, as it is blocked by pretreatment of cells with the pan-caspase inhibitor Z-VAD-FMK or by homozygous deletion of p53 (Supplementary Fig. 2c). To determine the degree of synergy between Nutlin-3 and ATMi, we treated cells with varying doses of each drug alone or in combination and measured the effects on cell viability (Supplementary Fig. 2d). These data were used to calculate combination indices (CI) using the Chou-Talalay Method[27], which revealed synergism at all combinations tested (i.e. CI<1). Various dose combinations produce CI values below 0.5, indicating strong synergy (Fig. 4e). Of note, there is a clear correlation between the effects of ATMi on cell viability and the degree of ATM inhibition as seen by Western blots against phospho-ATM (Supplementary Fig. 2d,e). Next, we utilized a 3D multicellular tumor spheroid (MCTS) model to examine this drug interaction under more physiological conditions. MCTSs are an intermediate between traditional cell culture and whole animal studies. MCTSs have gene expression profiles more similar to clinical samples than their 2D counterparts and are able to recapitulate other important characteristics of the tumor microenvironment including hypoxia, cell-cell and

cell-matrix interactions, and metabolic gradients[28]. Cells were plated on Matrigel for one week to allow spheroid formation and treated for three weeks with DMSO, Nutlin-3, ATMi or combination. As expected, vehicle treatment allows spheroid growth to continue while Nutlin-3 treatment results in growth arrest (Fig. 4f). Strikingly, while ATMi treatment allows continued MCTS growth, the combination of Nutlin-3 and ATMi results in almost complete ablation of all spheroids present.

Overall, these results demonstrate that the ATM pathway is required for survival of tumor cells upon non-genotoxic activation of p53 by Nutlin-3 and that ATM protects cells from p53-dependent apoptosis in this context.

MET inhibition promotes p53-induced apoptosis

The MET pathway was also highlighted by IPA as a top pathway of synthetic lethality with Nutlin-3 (Fig. 3c). MET (mesenchymal-epithelial transition factor), also known as hepatocyte growth factor receptor (HGFR), is a receptor tyrosine kinase frequently hyperactivated in many cancers, including colorectal carcinomas and non-small cell lung cancers (NSCLC)[22,29]. Other SLNs within the MET signaling node include PI3K (PIK3CD), SHP2 (PTPN11) and members of the downstream MAPK cascade MEK4 (MAP2K4) and JNK2 (MAPK9) (Fig. 3a,c). The synthetic lethal interaction between MET and Nutlin-3-activated p53 was validated with several shRNAs distinct from those used in the screen. In fact, eight different hairpins that reduce MET levels also decrease cell viability upon Nutlin-3 treatment (Supplementary Fig. 4a). As is the case for ATM, MET knockdown with different shRNAs leads to increased apoptotic indices upon Nutlin-3 treatment (Fig. 5a **and** Supplementary Fig. 4b). Importantly, overexpression of V5-tagged MET in cells expressing an shRNA targeting the 3′ UTR of the MET transcript produces a significant rescue of the synthetic lethal phenotype (Supplementary Fig. 4b). MET knockdown also leads to increased apoptosis in Nutlin-3-treated A549 cells (Supplementary Fig. 3). Next, we tested the effects of PF-02341066 (Crizotinib), a MET inhibitor approved for clinical use[30]. In fact, MET inhibition results in activation of caspases only when combined with Nutlin-3 (Fig. 5b) and induces cell death that is both caspase- and p53-dependent (Supplementary Fig. 4c). As with ATM inhibition, the MET inhibitor displays strong synergism with Nutlin-3. Relative viability drops off sharply with increased doses of Crizotinib and this effect is strongly exacerbated by addition of Nutlin-3 (Supplementary Fig. 4d). CI values for the Nutlin-3-Crizotinib interaction reveal a high degree of synergy (CI <0.2) in the majority of dosage combinations tested (Fig. 5c). We next tested the effects of Crizotinib in the MCTS assay. While Crizotinib alone has little effect on the growth of the tumor spheres, the combination treatment completely ablates them (Fig. 5d). Crizotinib has been found to inhibit other kinases beyond MET, such as ALK[31]. Although HCT116 cells do not express ALK, we decided nonetheless to confirm the specificity of the MET-p53 interaction with a structurally different MET inhibitor, SU11274[32]. In fact, SU11274 treatment leads to increased apoptosis upon Nutlin-3 treatment (Supplementary Fig. 4e). As expected, both Crizotinib and SU11274 strongly inhibit MET autophosphorylation in HCT116 cells (Supplementary Fig. 4f). Finally, we performed a side-by-side comparison of [Nutlin-3 + ATMi] and [Nutlin-3 + Crizotinib] combinations in six different Nutlin-3-resistant cell lines: RKO (colon cancer), A549 (lung adenocarcinoma), H460 (NSCLC),

U2OS (osteosarcoma), MCF7 (breast adenocarcinoma) and H226 (lung squamous cell carcinoma). All six cell lines show increased apoptosis with either combination treatment; however, the degree of synthetic lethality is variable (Fig. 5e). For example, whereas RKO and H460 cells show strong combinatorial effects, in U2OS and H226 cells the results are less striking due to heightened sensitivity to Crizotinib treatment alone.

Taken together, these results demonstrate that MET influences cell fate choice upon p53 activation and that inhibition of MET is sufficient to convert Nutlin-3-induced cell cycle arrest into apoptosis in several cancer cell types.

Parallel action of synthetic lethal pathways

Having successfully identified SLN pathways, we next investigated their regulation and mechanism of action. First, we employed a systems-wide approach to test if differential regulation of SLN pathways could explain the distinct phenotypes produced by p53 activation by Nutlin-3 versus the traditional genotoxic agent 5FU. As mentioned before, treatment of HCT116 cells with the anti-metabolite 5FU results in robust p53-dependent apoptosis[19] (Fig. 1d). Intriguingly, whereas Nutlin-3 and 5FU produce equivalent activation of p53 and PUMA, only 5FU leads to activation of executioner caspase 3 (Fig. 1e). Presumably, the pleiotropy of 5FU treatment triggers additional pro-apoptotic events that complement activation of the p53-PUMA axis to tip cells into apoptosis, and these hypothetical events would not be elicited by Nutlin-3. We sought to exploit this model of stimulus-specific cell fate choice to inform our SLN screen. We reasoned that a subset of our SLNs, which can be viewed as pro-survival genes, would be upregulated by Nutlin-3 and down-regulated by 5FU and that this differential regulation could potentially explain how cell fate choice is determined (Supplementary Fig. 5a). To test this, we performed microarray gene expression analysis of HCT116 cells treated with Nutlin-3 or 5FU. Interestingly, SLNs as a group were largely members of pathways parallel to p53, in the sense that very few of them displayed significant changes in mRNA expression after Nutlin-3 or 5FU treatment (Supplementary Fig. 5b,c). Surprisingly, not a single one of the top ~500 SLNs in HCT116 cells showed concomitant induction by Nutlin-3 and repression by 5FU. In fact, only one SLN was repressed only by 5FU and three activated only by Nutlin-3, but none of these showed both types of regulation.

Of note, MET itself has been reported to be a p53 target gene[33]; however, we found no substantial changes in MET expression at either the mRNA or protein levels upon Nutlin-3 in HCT116 cells (Supplementary Fig. 6a, b). Interestingly, we did find that MET expression correlates with cell type-specific responses to Nutlin-3. Whereas MET is highly expressed in HCT116 and A549 Nutlin-3-resistant cells, it is strongly silenced in BV173 Nutlin-3-sensitive cells (Supplementary Fig. 6c, d). In contrast, this correlation is not observed for ATM (Supplementary Fig. 6e, f).

Overall, these observations indicate that the alternative p53-dependent responses elicited by Nutlin-3 and 5FU in HCT116 cells are not due to differential regulation of SLN pathways at the mRNA level. Of course, it remains possible that the protein products encoded by SLNs are differentially regulated by mechanisms that do not alter mRNA expression. Assessment of this regulation is outside the scope of this study but will be addressed in future work.

ATM and MET inhibitors do not affect key p53 target genes

To further investigate the mechanism of synthetic lethality, we asked whether the apoptotic phenotype observed with the different drug combinations required the BH3-only protein PUMA, a key mediator of p53-dependent cell death that functions as a potent inhibitor of BCL2 survival factors and direct activator of the pore protein BAX[34]. Importantly, we observed that deletion of both alleles of *PUMA* abolishes the synthetic lethal phenotype of [Nutlin-3 + ATMi] and [Nutlin-3 + Crizotinib] combinations in HCT116 spheroids (Fig. 6a). Thus, PUMA is required for synthetic lethality. Of note, p53-dependent activation of p21 and 14-3-3σ, the key mediators of p53-induced cell cycle arrest, has been shown to attenuate p53/PUMA-dependent apoptosis in response to genotoxic agents[35]. Therefore, we hypothesized that SLN pathways may alter cell fate choice by affecting the transactivation of the key p53 target genes mediating each response. Interestingly, expression of p21, 14-3-3σ, PUMA, BAX and BCL2 is similar between cells treated with Nutlin-3 alone versus the combination treatments with ATM and MET inhibitors (Fig. 6b). However, only the combination treatments lead to cleavage of caspase 8 and appearance of truncated BID (tBID). Importantly, we have found that caspase 8 and BID are required for 5FU-induced apoptosis in this cell line[36]. To confirm that none of the drug treatments affected the ability of p53 to transactivate the key target genes in each pathway, we measured mRNA accumulation by quantitative RT-PCR. In fact, neither ATMi nor Crizotinib have an impact on induction of p21, PUMA or MDM2 by Nutlin-3-activated p53 (Fig. 6c).

In summary, these data demonstrate that SLN pathways act largely in a 'parallel fashion', in the sense that they govern the choice between cell cycle arrest and apoptosis without affecting the key p53 target genes previously involved in each response.

53BP1 is not required for ATM synthetic lethality

Our discovery that ATM antagonizes p53-dependent apoptosis in the context of non-genotoxic p53 activation contrasts with the established role of ATM as a p53 agonist during the DNA damage response[37]. Furthermore, a previous genetic screen identified 53BP1, a canonical component of ionizing radiation-induced foci, as required for Nutlin-3 to exert its anti-proliferative effects in MCF7 cells[38]. These observations lead us to ask whether ATM and 53BP1 act autonomously during non-genotoxic p53 activation. To test this we created cell lines stably expressing different shRNAs targeting 53BP1 and compared their behavior to that of ATM-depleted cells. Consistent with previous findings[38], we found that cells with reduced levels of 53BP1 have increased viability upon Nutlin-3 treatment; however, ATM knockdown clearly has the opposite effect (Fig. 7a,b). Furthermore, we found that 53BP1 knockdown does not block apoptosis induced by the [Nutlin-3+ATMi] combination (Fig. 7c).

Taken together, these results indicate that ATM synthetic lethality with Nutlin-3-activated p53 does not require 53BP1. Although ATM and 53BP1 may act coordinately in the DNA damage response, there is now ample evidence for a role of ATM in other signaling networks[39–41]. Therefore, our findings reveal an unexpected role for ATM during non-genotoxic p53 activation.

DISCUSSION

p53 has been an unwitting target of traditional cancer therapeutics since the development of radiotherapy and genotoxic chemotherapy. These treatments rely on the cellular DNA damage response for success, which is why they are often less effective in the ~50% of cancers with mutant p53. A recent flurry of drug discovery efforts has identified cleaner and safer strategies to harness the tumor suppressive power of p53 for selective elimination of cancer cells. This growing list includes targeted therapeutics such as Nutlin-3, which binds to and blocks MDM2; PRIMA-1[42], which reactivates mutant p53; and RITA[43], which binds directly to p53 and stabilizes it. However, the clinical worth of these drugs is limited *a priori* by the pleiotropic character of the p53 network. Depending on the context, p53 can promote survival or death. The key question then becomes: what determines the cellular response to p53 activation? We have employed Nutlin-3 as a paradigm to answer this question. Nutlin-3 elicits cell cycle arrest or apoptosis in a cell-type specific manner[6,8]. Our functional genomics approach has successfully identified gene modules that enforce survival in Nutlin-3-resistant cells. This has led us not only to a greater understanding of the p53 network, but also to the identification of new combinatorial strategies to augment the therapeutic efficacy of Nutlin-3.

Our identification of ATM as an antagonist of p53 dependent-apoptosis was totally unexpected. Current dogma maintains that ATM activates p53 in response to DNA damage by phosphorylating specific serines in both p53 and MDM2, thus preventing their interaction and leading to p53 stabilization[44]. According to this view, ATM functions as a p53 agonist during the apoptotic response to DNA damage[37]. However, a uniform view of ATM in the response to genotoxic therapies is prevented by the observation that ATM has also been shown to activate pro-survival pathways upon DNA damage, such as the NF-κB pathway[41,45]. In fact, the role of ATM can be switched from pro-survival to pro-apoptotic depending on the extent of DNA damage[39]. As mentioned above, radiation and genotoxic drugs have been widely used in the clinic for years. One strategy to increase the efficacy of these treatments has been to target components of the DNA damage repair machinery. As such, inhibitors of upstream signaling kinases in these pathways (e.g. ATM, ATR, DNA-PK) have been employed to confer radio- and/or chemo-sensitivity upon cancer cells[46]. Unfortunately, many of the known inhibitors of these kinases, including wortmannin and caffeine, lack specificity and inhibit a wide range of PI3K-like kinases[46]. The development of KU-55933 imparts specificity on this system, targeting ATM with a much lower IC50 than previous inhibitors[26]. However, even specific inhibitors would still rely on the introduction of high levels of DNA damage and its associated pleiotropic effects. Our finding that a combination of non-genotoxic p53 activation and ATM inhibition is capable of eliciting an apoptotic response in cancer cells is a conceptual breakthrough, as it does not induce a DNA damage response above stochastic levels, which is already high in tumors. This is the first report showing that ATM is required for survival upon pharmacological activation of p53 in the absence of exogenously introduced DNA damage. Future studies will investigate how exactly ATM promotes its anti-apoptotic effects in this scenario.

Our 53BP1 studies provide additional support for the notion that ATM activity can be decoupled from other components of the DNA damage response pathway. Previous work

showed that 53BP1 knockdown allows cells to escape Nutlin-3-induced cell cycle arrest and impairs Nutlin-3-induced upregulation of p21[38]. We confirm a role for 53BP1 in the anti-proliferative effects of Nutlin-3, and, conversely, show that ATM inhibition converts cell cycle arrest into apoptosis without affecting expression of p21. In this report the authors did not test the role of ATM directly, but used caffeine, a broad inhibitor of PI3Ks, which suggested that one or more PI3Ks were required for full induction of p21 and cell cycle arrest in their system. However, they used a cell line (MCF7) displaying constitutive DNA damage signaling as seen by H2A.X foci, and a dose of Nutlin-3 that did not produce maximum induction of p21. In contrast, our screen was performed in cells with no apparent constitutive DNA damage signaling and with a dose of Nutlin-3 that leads to maximum p21 induction. Thus, while their screen was prone to identify a role for DNA damage signaling in complementing pharmacological inhibition of MDM2 for cell cycle arrest, ours was not.

The MET network plays an important role in many malignancies. Upon activation by HGF, MET activates various intracellular pathways promoting proliferation, survival, and invasion[47]. MET is hyperactivated or overexpressed in many cancers, making it an attractive target for therapeutic intervention[22,29,47]. Crizotinib was originally developed as a MET-specific inhibitor[30], however, it also inhibits ALK (anaplastic lymphoma kinase)[31]. ALK is a receptor tyrosine kinase within the insulin-receptor superfamily with roles in development and function of the nervous system[31]. However, ALK is not essential, as knockout mice are viable and mostly normal[31]. ALK is frequently translocated in lung cancer[48]. Crizotinib underwent clinical trials for NSCLC patients with MET amplification or ALK translocations, which ultimately determined that in this case cancers with ALK translocations were better targets for Crizotinib[49]. We show here that Crizotinib sensitizes cells to p53-induced cell death. This strongly implicates the MET pathway in survival signaling upon p53 activation, as none of the cell lines used in this study has ALK translocations or detectable ALK expression (Cancer Cell Line Project, Welcome Trust Sanger Institute). Furthermore, we found that a second MET inhibitor, SU11274[32], also sensitizes to Nutlin-3-induced apoptosis. Interestingly, although MET has been depicted as a target of p53 repression[33], we did not observe changes in MET expression upon non-genotoxic activation of p53 in Nutlin-3-resistant cells. However, we found that MET is strongly silenced in BV173 cells, which could partially explain why they undergo apoptosis upon Nutlin-3 treatment. These results not only reveal a new functional module affecting outcome to p53 activation, but demonstrate the ability of synthetic lethal screens to resuscitate drugs that may not have been effective as single agents, despite the great time and cost spent on their development.

Much of the research on mechanisms of cell fate choice to p53 activation has focused on p53-centric events, such as p53 post-translational modifications, p53-binding factors and regulation of p53 DNA binding activity. The overarching view generated by these studies is that cell fate choice is determined by differential transactivation of p53 target genes involved in cell cycle arrest (e.g. p21, 14-3-3σ) versus apoptosis (e.g. PUMA)[1,17]. In contrast, our functional genomics approach revealed that the p53 response can be converted from cell cycle arrest into apoptosis without affecting expression of these key genes. Therefore, our results reinforce an alternative model where cell fate choice to p53 activation is governed by p53 autonomous mechanisms[8,18,36]. This alternative view is more consistent with our

increasing appreciation of cancer as disease of gene networks, rather than individual gene modules or linear pathways.

Although we focused our efforts on two key pathways, ATM and MET, we are fully aware that many other relevant SLN pathways identified in our screen remain unexplored. We hope that making the results of our screen available to the community will inspire other teams to identify additional strategies to modulate the p53 response for therapeutic purposes and to generate a greater understanding of the p53 network.

METHODS

Cell culture, lentiviral work and drug treatments

HCT116 and RKO cells were cultured in McCoy's 5A Medium, A549 and H460 cells in DMEM/F12, BV173 and H460 cells in RPMI-1640 and HEK293FT, MCF7 and U2OS cells were cultured in DMEM. Media was supplemented with 10% FBS and antibiotic/ antimycotics. SBI library production was performed by transfecting 4 μg of SBI library plasmid into HEK293T cells for 48 hours. Viral supernatant was used to transduce HCT116 and A549 cells with polybrene. shRNA cell lines were produced by linear PEI transfection of HEK293FT cells with pLKO vectors for 48 hours followed by 24 hours transduction with polybrene (see Supplementary Dataset 5 for shRNA sequences). Transduced cells were selected with 10 μg/mL puromycin (Sigma-Aldrich, >98% purity). Nutlin-3 ((±)-4-[4,5-bis-(4-chlorophenyl)-2-(2-isopropoxy-4-methoxy-phenyl)-4,5-dihydro-imidazole-1-carbonyl]-piperazin-2-one, Cayman, >98% purity), 5FU (5-Fluoro-2,4-(1H,3H)-pyrimidinedione, Sigma-Aldrich, >99% purity), ATMi/KU55933 (2-(4-Morpholinyl)-6-(1-thianthrenyl)-4H-pyran-4-one, Tocris, >98% purity), Crizotinib/PF-02341066 ((R)-3-[l-(2,6-Dichloro-3 - fluorophenyl)ethoxy]-5- [1-(piperidin-4-yl)- 1H-pyrazol-4-yl]pyridin-2-amine, Tocris, >99% purity), SU11274 ((3Z)-N-(3-Chlorophenyl)-3-({3,5-dimethyl-4-[(4-methylpiperazin-1-yl)carbonyl]-1H-pyrrol-2-yl}methylene)-N-methyl-2-oxo-2,3-dihydro-1H-indole-5-sulfonamide, Tocris, >99% purity) and Z-VAD-FMK (Benzyloxycarbonyl-Val-Ala-Asp(OMe)-fluoromethylketone, Tocris, >95% purity) were solubilized in DMSO and cells treated with indicated concentrations for the indicated times.

Deep sequencing of shRNAs

Total RNA was harvested by Trizol extraction and reverse transcribed using the iScript cDNA synthesis kit (BioRad) and the vector specific GNH primer supplied by SBI. The cDNA was PCR amplified using Fwd and Rev GNH primers from SBI, followed by a nested reaction with custom primers to add Illumina specific sequences (GNH-ISS) (see Supplementary Table 1 for primer sequences). Final PCR products were purified with the QIAquick PCR purification kit (Qiagen) and quantified with NanoDrop. 0.5 pMoles were sequenced on a Genome Analyzer$_{II}$ according to manufacturer's instructions using a customized sequencing primer (CSP-GNH).

In Silico Work: BiNGS

Image data from Genome Analyzer$_{II}$ was processed for base calling, quality analysis and quantification using Illumina software. All targeting sequences from shRNAs in the SBI

library were mapped to the human reference genome (RefSeq GRch37, hg19) with Bowtie to identify the gene target for each shRNA and thus create an 'SBI Reference Library'. To analyze the screen data we employed BiNGS, which was developed for this purpose[20]. BiNGS consists of five analytical steps including: 1) pre-processing, 2) mapping, 3) statistical analysis, 4) post-analysis and 5) pathway analysis. Preprocessing filters out erroneous and low quality reads. Mapping aligns shRNAs sequenced during the screen to the SBI Reference Library using Bowtie, generating a $P \times N$ matrix where P and N are the read counts and samples, respectively. A second filtering step then removes shRNAs mapped to unannotated sequences. Our statistical model is a Negative Binomial to model the count distribution in the sequencing data using edgeR. After edgeR, we filtered out shRNAs where the median count of the control group is lower than the maximum count of the treatment group and vice versa to eliminate shRNA tags with high variability in counts, lowering the rate of false positives. We compute the q-value of false discovery rate for multiple comparisons of these shRNAs in order to calculate the adjusted p values. Post-analysis consists of Meta-analysis where the adjusted p-values of all shRNAs targeting a single gene are combined using a weighted Z-transformation that puts weight on small adjusted p-values. This method allows us to collapse multiple shRNAs per gene, generating an associated p-value (p(wZ)). When several shRNAs for a given gene show concurrent synthetic lethality, the p(wZ) value becomes very small to reflect this increased confidence. This method does not normalize to the number of shRNAs in the initial input SBI library, but it does take into account all shRNAs for a given gene detected during the experiment (i.e. all shRNAs counted in DMSO- and/or Nutlin-3 treatments). Results are shown in Supplementary Dataset 1–4. The selection of the 30 genes validated in Fig. 2e was based on various measurements which contribute to the p(wZ) value, including single hairpins with the greatest fold change in either HCT116 or A549 (e.g. *MED21* and *MON1B*), greatest number of strongly scoring hairpins (e.g. *SRPK1* and *MADCAM1*) and the absolute p(wZ) value itself (e.g. *CCND1* and *MACF1*). We also selected genes based on Ingenuity Pathway Analysis (e.g. *ATM* and *MET*) as well as known p53 target genes (e.g. *CAV1* and *VDR*).

Microarray Analysis

RNA was harvested from cells treated with Nutlin-3, 5FU, or DMSO for 12 hours using the RNeasy kit (Qiagen). cDNAs were synthesized and labeled with the Genechip Whole Transcript Sense Target Labeling Kit (Affymetrix) per the manufacturer's instructions and hybridized to Human Exon 1.0 ST arrays (Affymetrix). Raw signals from the microarrays were extracted and normalized by Robust Multiarray Analysis (RMA). All experiments were performed in duplicate. Differentially expressed genes were identified using ANOVA in the Partek Genomic Suite. Data were deposited in Gene Expression Omnibus with accession number GSE36593.

SRB assay

Cells were fixed with 3.3% TCA for 1 hour at 4°C, washed 4 times with dH$_2$O and stained with 0.057% (w/v) sulforhodamine B (SRB) in 1% acetic acid for 30 min at 4°C. Cells were then washed 4 times with 10% acetic acid and allowed to air dry. SRB was eluted in 10 mM Tris-base pH 10.5 and quantified with a Synergy2 (Biotek) plate reader at 590 nm.

MCTS Assay

5×10^3 HCT116 cells in 2% Matrigel were plated into each well of an 8-chambered slide pre-coated with Matrigel. Cells were grown for seven days without treatment to allow for spheroid formation. Subsequently, cells were treated with drugs in complete media containing 2% Matrigel and their progress monitored for up to 28 days.

Crystal Violet Staining

Cells were fixed in 4% paraformaldehyde in PBS for 15 min at 25°C. After washing with dH$_2$O, fixed cells were stained with 0.1% (w/v) crystal violet in 10% ethanol for 20 min at 25°C. Stained cells were washed with dH$_2$O and air dried prior to imaging.

Flow Cytometry, Western Blots and Q-RT-PCR

Western blots and Q-RT-PCR performed as previously described[8]. For antibodies and primer sequences see Supplementary Tables 1 and 2, respectively.

MET cloning

pDONR223-MET was acquired from Addgene (plasmid 23889, deposited by William Hahn and David Root) and Gateway cloned into pcDNA3.1/nV5-DEST.

Supplementary Material

Refer to Web version on PubMed Central for supplementary material.

Acknowledgments

References

1. Vousden KH, Prives C. Blinded by the Light: The Growing Complexity of p53. Cell. 2009; 137:413–31. [PubMed: 19410540]

2. Brown CJ, Lain S, Verma CS, Fersht AR, Lane DP. Awakening guardian angels: drugging the p53 pathway. Nat Rev Cancer. 2009; 9:862–73. [PubMed: 19935675]

3. Levesque AA, Eastman A. p53-based cancer therapies: Is defective p53 the Achilles heel of the tumor? Carcinogenesis. 2007; 28:13–20. [PubMed: 17088261]

4. Mandinova A, Lee SW. The p53 pathway as a target in cancer therapeutics: obstacles and promise. Sci Transl Med. 2011; 3:64rv1.

5. Vassilev LT, et al. In vivo activation of the p53 pathway by small-molecule antagonists of MDM2. Science. 2004; 303:844–8. [PubMed: 14704432]

6. Tovar C, et al. Small-molecule MDM2 antagonists reveal aberrant p53 signaling in cancer: implications for therapy. Proc Natl Acad Sci U S A. 2006; 103:1888–93. [PubMed: 16443686]

7. Huang B, Deo D, Xia M, Vassilev LT. Pharmacologic p53 activation blocks cell cycle progression but fails to induce senescence in epithelial cancer cells. Mol Cancer Res. 2009; 7:1497–509. [PubMed: 19737973]

8. Paris R, Henry RE, Stephens SJ, McBryde M, Espinosa JM. Multiple p53-independent gene silencing mechanisms define the cellular response to p53 activation. Cell Cycle. 2008; 7:2427–33. [PubMed: 18677110]

9. Ventura A, et al. Restoration of p53 function leads to tumour regression in vivo. Nature. 2007; 445:661–5. [PubMed: 17251932]

10. Xue W, et al. Senescence and tumour clearance is triggered by p53 restoration in murine liver carcinomas. Nature. 2007; 445:656–60. [PubMed: 17251933]

11. el-Deiry WS, et al. WAF1, a potential mediator of p53 tumor suppression. Cell. 1993; 75:817–25. [PubMed: 8242752]

12. Hermeking H, et al. 14-3-3 sigma is a p53-regulated inhibitor of G2/M progression. Mol Cell. 1997; 1:3–11. [PubMed: 9659898]

13. Yu J, Zhang L, Hwang PM, Kinzler KW, Vogelstein B. PUMA induces the rapid apoptosis of colorectal cancer cells. Mol Cell. 2001; 7:673–82. [PubMed: 11463391]

14. Nakano K, Vousden KH. PUMA, a novel proapoptotic gene, is induced by p53. Mol Cell. 2001; 7:683–94. [PubMed: 11463392]

15. Wu GS, et al. KILLER/DR5 is a DNA damage-inducible p53-regulated death receptor gene. Nat Genet. 1997; 17:141–3. [PubMed: 9326928]

16. Muller M, et al. p53 activates the CD95 (APO-1/Fas) gene in response to DNA damage by anticancer drugs. J Exp Med. 1998; 188:2033–45. [PubMed: 9841917]

17. Vousden KH, Lu X. Live or let die: the cell's response to p53. Nat Rev Cancer. 2002; 2:594–604. [PubMed: 12154352]

18. Sullivan KD, Gallant-Behm CL, Henry RE, Fraikin JL, Espinosa JM. The p53 circuit board. Biochim Biophys Acta. 2012; 1825:229–44. [PubMed: 22333261]

19. Bunz F, et al. Disruption of p53 in human cancer cells alters the responses to therapeutic agents. J Clin Invest. 1999; 104:263–9. [PubMed: 10430607]

20. Kim J, Tan AC. BiNGS!SL-seq: a bioinformatics pipeline for the analysis and interpretation of deep sequencing genome-wide synthetic lethal screen. Methods Mol Biol. 2012; 802:389–98. [PubMed: 22130895]

21. Porter CC, et al. Integrated genomic analyses identify WEE1 as a critical mediator of cell fate and a novel therapeutic target in acute myeloid leukemia. Leukemia. 201210.1038/leu.2011.392

22. Di Renzo MF, et al. Overexpression and amplification of the met/HGF receptor gene during the progression of colorectal cancer. Clin Cancer Res. 1995; 1:147–54. [PubMed: 9815967]

23. Takhar AS, Eremin O, Watson SA. The role of gastrin in colorectal carcinogenesis. Surgeon. 2004; 2:251–7. [PubMed: 15570843]

24. Li A, Varney ML, Singh RK. Expression of interleukin 8 and its receptors in human colon carcinoma cells with different metastatic potentials. Clin Cancer Res. 2001; 7:3298–304. [PubMed: 11595728]

25. Sugai T, et al. Frequent allelic imbalance at the ATM locus in DNA multiploid colorectal carcinomas. Oncogene. 2001; 20:6095–101. [PubMed: 11593417]

26. Hickson I, et al. Identification and characterization of a novel and specific inhibitor of the ataxia-telangiectasia mutated kinase ATM. Cancer Res. 2004; 64:9152–9. [PubMed: 15604286]

27. Chou TC. Drug combination studies and their synergy quantification using the Chou-Talalay method. Cancer Res. 2010; 70:440–6. [PubMed: 20068163]

28. Friedrich J, Seidel C, Ebner R, Kunz-Schughart LA. Spheroid-based drug screen: considerations and practical approach. Nat Protoc. 2009; 4:309–24. [PubMed: 19214182]

29. Olivero M, et al. Overexpression and activation of hepatocyte growth factor/scatter factor in human non-small-cell lung carcinomas. Br J Cancer. 1996; 74:1862–8. [PubMed: 8980383]

30. Yamazaki S, et al. Pharmacokinetic-pharmacodynamic modeling of biomarker response and tumor growth inhibition to an orally available cMet kinase inhibitor in human tumor xenograft mouse models. Drug Metab Dispos. 2008; 36:1267–74. [PubMed: 18381487]

31. Shaw AT, Solomon B. Targeting anaplastic lymphoma kinase in lung cancer. Clin Cancer Res. 2011; 17:2081–6. [PubMed: 21288922]

32. Sattler M, et al. A novel small molecule met inhibitor induces apoptosis in cells transformed by the oncogenic TPR-MET tyrosine kinase. Cancer Res. 2003; 63:5462–9. [PubMed: 14500382]

33. Hwang CI, et al. Wild-type p53 controls cell motility and invasion by dual regulation of MET expression. Proc Natl Acad Sci U S A. 2011; 108:14240–5. [PubMed: 21831840]

34. Zhang Y, Xing D, Liu L. PUMA promotes Bax translocation by both directly interacting with Bax and by competitive binding to Bcl-X L during UV-induced apoptosis. Mol Biol Cell. 2009; 20:3077–87. [PubMed: 19439449]

35. Chan TA, Hwang PM, Hermeking H, Kinzler KW, Vogelstein B. Cooperative effects of genes controlling the G(2)/M checkpoint. Genes Dev. 2000; 14:1584–8. [PubMed: 10887152]

36. Henry RE, Andrysik Z, Paris R, Galbraith MD, Espinosa JM. A DR4:tBID axis drives the p53 apoptotic response by promoting oligomerization of poised BAX. EMBO J. 2012; 31:1266–78. [PubMed: 22246181]

37. Jiang H, et al. The combined status of ATM and p53 link tumor development with therapeutic response. Genes Dev. 2009; 23:1895–909. [PubMed: 19608766]

38. Brummelkamp TR, et al. An shRNA barcode screen provides insight into cancer cell vulnerability to MDM2 inhibitors. Nat Chem Biol. 2006; 2:202–6. [PubMed: 16474381]

39. Biton S, Ashkenazi A. NEMO and RIP1 control cell fate in response to extensive DNA damage via TNF-alpha feed forward signaling. Cell. 2011; 145:92–103. [PubMed: 21458669]

40. Guo Z, Kozlov S, Lavin MF, Person MD, Paull TT. ATM activation by oxidative stress. Science. 2010; 330:517–21. [PubMed: 20966255]

41. Hadian K, Krappmann D. Signals from the nucleus: activation of NF-kappaB by cytosolic ATM in the DNA damage response. Sci Signal. 2011; 4:pe2. [PubMed: 21245467]

42. Bykov VJ, et al. Restoration of the tumor suppressor function to mutant p53 by a low-molecular-weight compound. Nat Med. 2002; 8:282–8. [PubMed: 11875500]

43. Issaeva N, et al. Small molecule RITA binds to p53, blocks p53-HDM-2 interaction and activates p53 function in tumors. Nat Med. 2004; 10:1321–8. [PubMed: 15558054]

44. Lavin MF. Ataxia-telangiectasia: from a rare disorder to a paradigm for cell signalling and cancer. Nat Rev Mol Cell Biol. 2008; 9:759–69. [PubMed: 18813293]

45. Miyamoto S. Nuclear initiated NF-kappaB signaling: NEMO and ATM take center stage. Cell Res. 2011; 21:116–30. [PubMed: 21187855]

46. Ding J, Miao ZH, Meng LH, Geng MY. Emerging cancer therapeutic opportunities target DNA-repair systems. Trends Pharmacol Sci. 2006; 27:338–44. [PubMed: 16697054]

47. Trusolino L, Bertotti A, Comoglio PM. MET signalling: principles and functions in development, organ regeneration and cancer. Nat Rev Mol Cell Biol. 2010; 11:834–48. [PubMed: 21102609]

48. Soda M, et al. Identification of the transforming EML4-ALK fusion gene in non-small-cell lung cancer. Nature. 2007; 448:561–6. [PubMed: 17625570]

49. Kwak EL, et al. Anaplastic lymphoma kinase inhibition in non-small-cell lung cancer. N Engl J Med. 2010; 363:1693–703. [PubMed: 20979469]
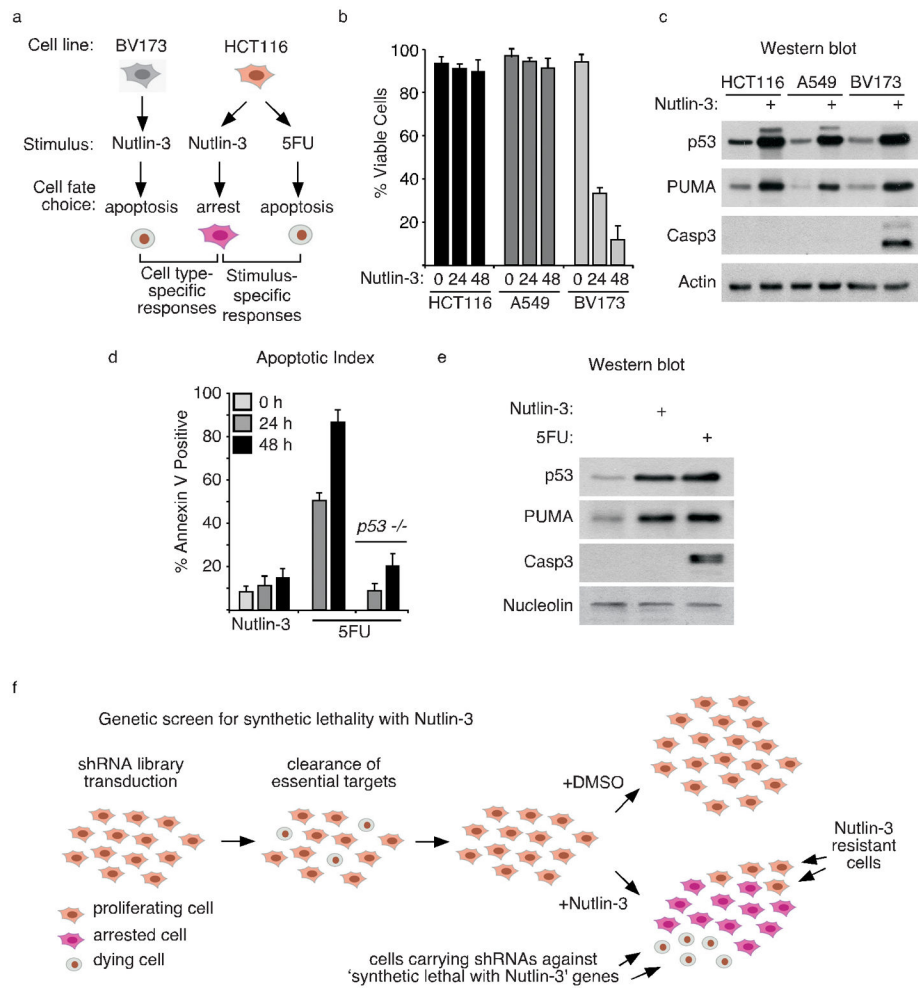
Figure 1. A genetic screen to identify modulators of the cellular response to p53 activation by Nutlin-3

(**a**) Experimental paradigms of cell type- and stimulus-specific p53-dependent cell fate choices used in this report. (**b**) Non-genotoxic activation of p53 by 20 μM Nutlin-3 leads to apoptosis only in select cell types. Relative viability of HCT116, A549 and BV173 cells as assessed by Annexin V and propidium iodide (PI) staining. (**c**) Nutlin-3 activates p53 and its pro-apoptotic target gene PUMA in all cell types tested, but activates executioner caspase 3 only in BV173 cells. Western blots for p53, PUMA and cleaved caspase 3 were performed on lysates prepared from cells treated with 20 μM Nutlin-3 or DMSO for 24 h. Actin serves as a loading control. Full blots can be found in Supplementary Fig. 7. (**d**) 5FU elicits a p53-dependent apoptotic response in HCT116 cells. Cells were treated with 5FU (375 μM) for the indicated period of time prior to Annexin V and PI analysis by flow cytometry. (**e**) Nutlin-3 (20 μM) and 5FU (375 μM) activate p53 and PUMA to similar levels, but only 5FU activates caspase 3. Lysates were prepared from cells treated with the indicated drug for 24 h and Western blots performed for p53, PUMA and cleaved caspase 3. Nucleolin serves as a loading control. (**f**) Schematic of genetic screen design.
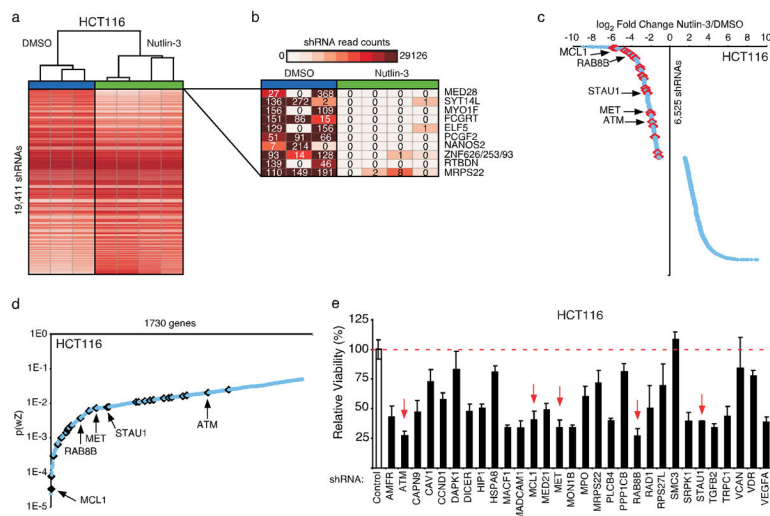
Figure 2. Identification of 'Synthetic Lethal with Nutlin-3' genes
(**a**) Hierarchical clustering analysis of raw sequence counts of shRNAs from HCT116 cells. Heatmap of 19,411 shRNAs where the median count of one treatment is greater than the maximum count of the other treatment. (**b**) Actual read counts of top 10 candidate SLN shRNAs. (**c**) Distribution of fold change for each shRNA with a p-value <0.05 (total of 6,525) from HCT116 cells. Red diamonds indicate the position of the 30 shRNAs chosen for validation in **e**. Arrows indicate the position of 5 shRNAs highlighted throughout the figure. (**d**) Distribution of 1730 genes from HCT116 cells with p(wZ) values <0.05. Black diamonds indicate positions of the 30 genes tested in **e**. (**e**) Validation of 30 predicted SLNs. Cell lines stably expressing single hairpins targeting the indicated gene were treated with 20 μM Nutlin-3 for 72 hours and analyzed by SRB assay. Relative viability was calculated as the ratio of Nutlin-3 treatment to DMSO treatment and compared to a non-targeting control shRNA. Data shown are an average of three experiments ± standard deviation.
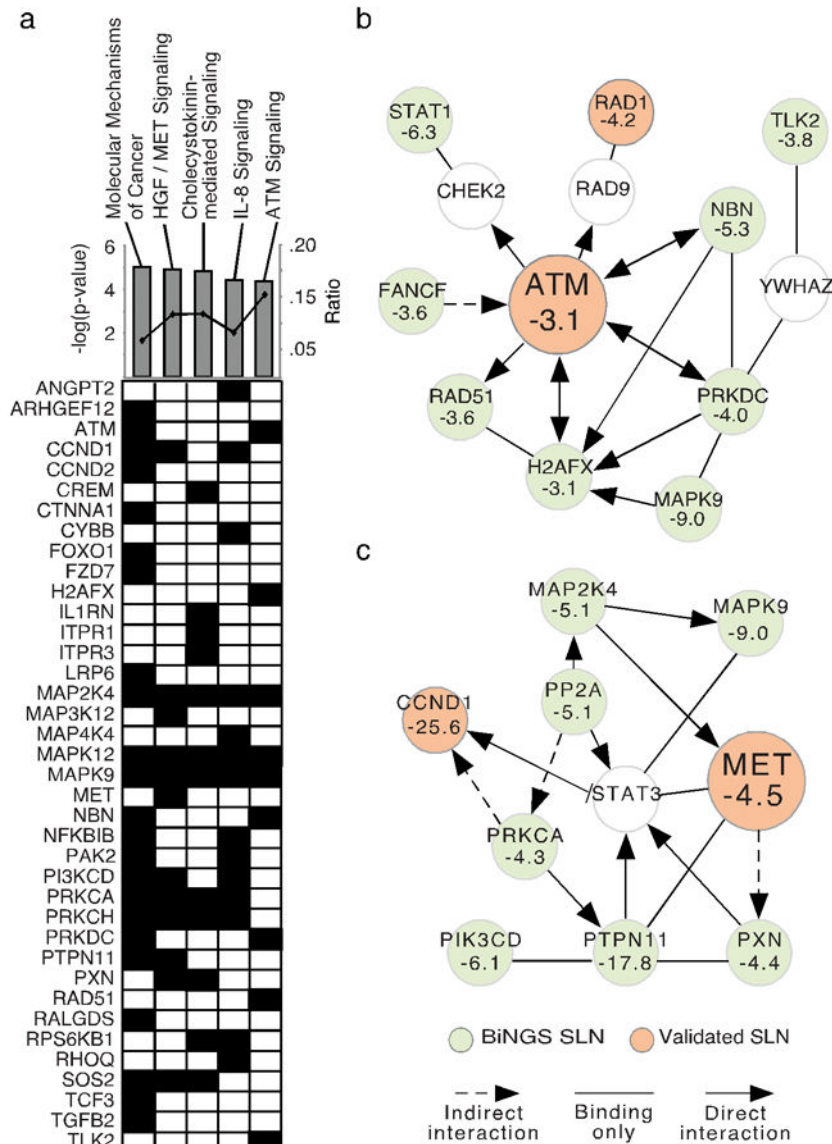
Figure 3. Pathway analysis points to ATM and MET as modulators of p53-dependent cell fate choice

(**a**) Top, the highest scoring 505 SLNs from HCT116 cells were analyzed using IPA software. The top five canonical pathways identified are shown. Gray bars represent enrichment p-value for corresponding pathway. Black line represents absolute ratio of genes from a given pathway that are SLNs. Bottom, matrix of SLNs from each pathway. Listed genes were identified as SLNs in the genome-wide screen. Black boxes indicate that a gene is a component of a given pathway. (**b**) ATM module. Orange balls represent validated SLN and green balls represent SLNs predicted by BiNGS. Numbers represent fold change in abundance of shRNA with greatest change from screen. (**c**) MET module. Analyzed as in **b**.
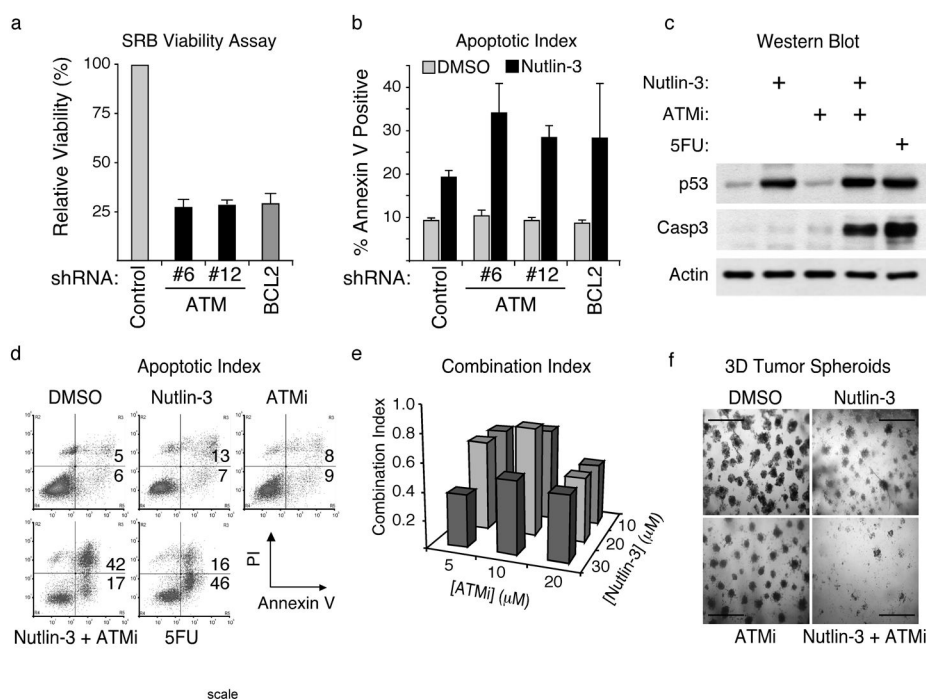
Figure 4. ATM protects cells from p53-dependent apoptosis upon Nutlin-3 treatment
(**a**) ATM knockdown impairs cell viability in response to Nutlin-3 treatment. Cell lines stably expressing shRNAs targeting ATM were treated with 20 μM Nutlin-3 for 72 h and analyzed as in **2e**. BCL2 serves as positive control. A non-targeting shRNA serves as a negative control. (**b**) ATM knockdown increases apoptosis upon Nutlin-3 treatment. Cell lines from **a** were treated with 20 μM Nutlin-3 or DMSO for 24 h prior to assessment of Annexin-V FITC and PI levels by flow cytometry. (**c**) Chemical inhibition of ATM activates executioner caspase 3 upon p53 activation by Nutlin-3. Lysates were prepared from cells treated with 10 μM ATMi, 20 μM Nutlin-3 and 375 μM 5FU for 24 h and Western blots performed for p53 and cleaved caspase 3. Actin serves as a loading control. Full blots can be found in Supplementary Fig. 7. (**d**) Treatment of cells with ATMi and Nutlin-3 results in robust apoptosis. Cells were treated with the indicated drugs as in **c** before Annexin V and PI levels were measured by flow cytometry. (**e**) The combination of ATMi and Nutlin-3 is highly synergistic. Cells were treated as in **c** for 24 h before SRB analysis. Combination index (CI) values were calculated using Calcusyn software. (**f**) Combination treatment is effective in a 3D culture system. HCT116 cells were plated on Matrigel pads for one week to allow tumor spheroid formation, then treated for 3 weeks before imaging. Scale bars, 1 mm.
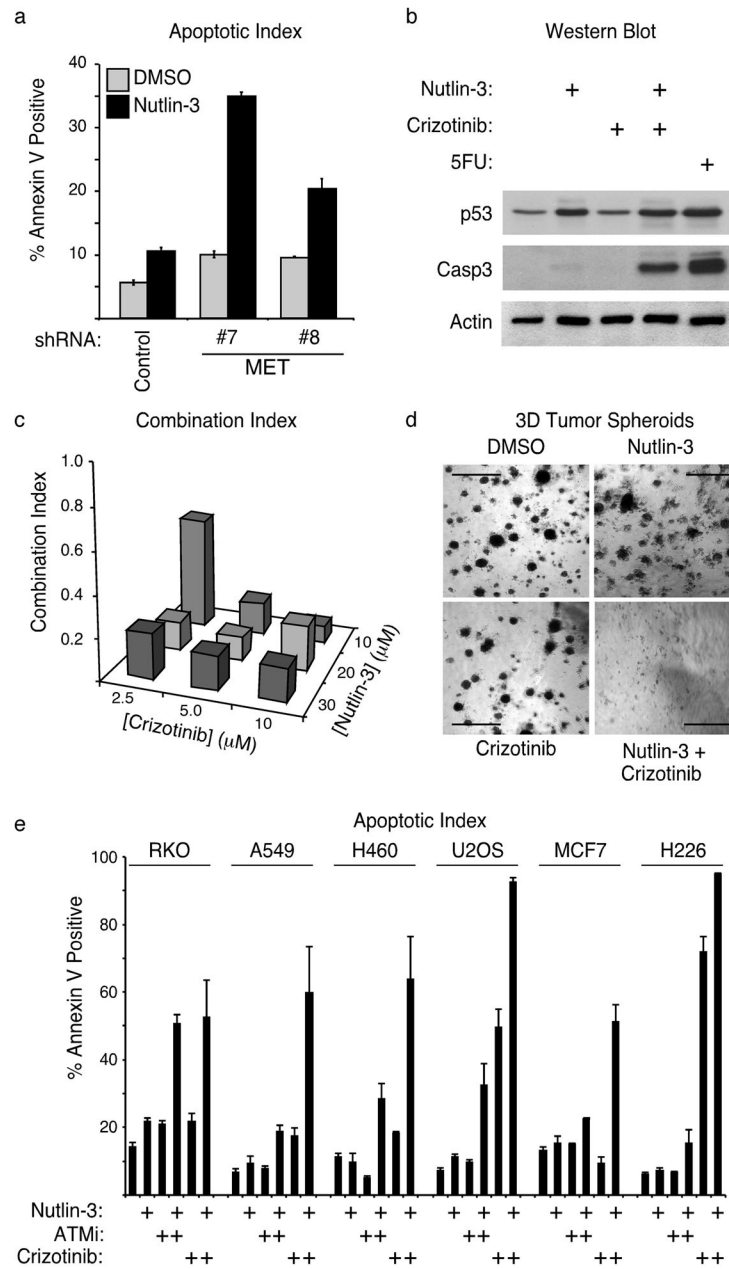
Figure 5. MET protects against p53-dependent apoptosis upon Nutlin-3 treatment
(**a**) MET knockdown leads to increased apoptosis upon Nutlin-3 treatment. Cell lines expressing indicated shRNAs were treated with 20 μM Nutlin-3 or DMSO for 24 h prior to assessment of Annexin-V FITC and PI levels by flow cytometry. (**b**) Crizotinib converts the cellular response to Nutlin-3 from cell cycle arrest to apoptosis in HCT116 cells. Lysates were prepared from cells treated with 7 μM Crizotinib, 20 μM Nutlin-3 and 375 μM 5FU for 24 h and Western blots performed for p53 and cleaved caspase 3. Actin serves as a loading control. Full blots can be found in Supplementary Fig. 7. (**c**) The combination of Crizotinib and Nutlin-3 is highly synergistic. CI values were calculated as in Fig. 4e. (**d**) Crizotinib and Nutlin-3 clear tumor spheroids effectively. Tumor spheres were prepared and treated as in

Fig. 4f for 12 days, at which point the combination treatment was devoid of viable cells. Scale bars, 1 mm. (**e**) Combinations of either ATMi or Crizotinib with Nutlin-3 increase the apoptotic index cancer cell types of different origins. Cells were treated with 10 μM ATMi, 7 μM Crizotinib and 20 μM Nutlin-3, for 24 h prior to analysis of Annexin V and PI by flow cytometry. Data shown are an average of three experiments ± standard deviation.
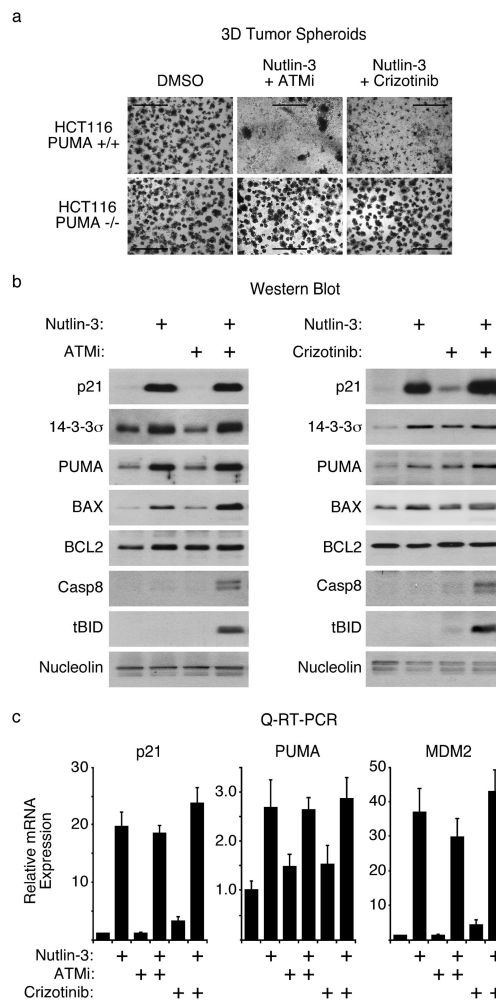
Figure 6. ATM and MET do not affect the ability of p53 to transactivate key genes in the cell cycle arrest and apoptosis modules

(**a**) PUMA is required for synthetic lethality of ATMi or Crizotinib in combination with Nutlin-3. Tumor spheres of HCT116 cells of different PUMA status were prepared as in Fig. 4f and treated with the indicated drug combinations for three weeks. Scale bars, 1 mm. (**b**) Neither ATMi nor Crizotinib affect protein expression of important p53-regulated cell cycle arrest or apoptotic target genes. Lysates were prepared from cells treated with 10 μM ATMi, 7 μM Crizotinib and 20 μM Nutlin-3, and expression of cell cycle arrest (p21 and 14-3-3σ), pro-apoptotic (PUMA and BAX), pro-survival (BCL2) and extrinsic apoptotic pathway (cleaved caspase 8 and tBID) proteins was analyzed by Western blot. Nucleolin serves as a loading control. Full blots can be found in Supplementary Fig. 7. (**c**) Drug combinations do not affect the transactivation ability of Nutlin-3-activated p53. RNA was harvested from cells treated with drugs as in **b** and Q-RT-PCR performed to test induction of p21, PUMA and MDM2 mRNAs.
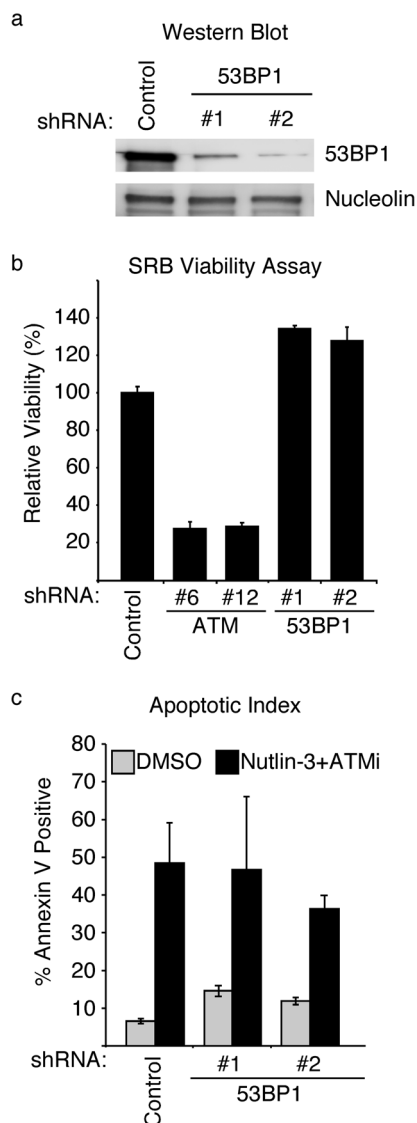
Figure 7. 53BP1 is not required for ATM synthetic lethality
(**a**) Western blot of 53BP1 knockdown cell lines. Nucleolin serves as a loading control. Full blots can be found in Supplementary Fig. 7. (**b**) In contrast to ATM knockdown, 53BP1 knockdown increases cell viability in response to Nutlin-3 treatment. Cell lines stably expressing shRNAs targeting ATM or 53BP1 were treated with 20 μM Nutlin-3 for 72 hours prior to analysis by SRB staining. (**c**) 53BP1 knockdown does not block apoptosis in response to [Nutlin-3+ATMi]. Cell lines expressing either control or 53BP1 shRNAs were treated with the indicated drugs prior to assessment of Annexin-V-FITC staining by flow cytometry.